

Reprinted from

GEODERMA

Geoderma 73 (1996) 63–82

Petrological differentiation patterns and geomorphic distribution of ferricretes in Central Africa

Anicet Beauvais^{a,*}, Claude Roquin^b

^a *Institut Français de Recherche Scientifique pour le Développement en Coopération (ORSTOM), UR12-TOA, 32 Avenue Henri Varagnat, 93143 Bondy Cedex, France*

^b *Centre de Géochimie de la Surface, UPR 6251 C.N.R.S, Institut de Géologie, 1, rue Blessig, 67084 Strasbourg Cedex, France*

Received 24 May 1995; accepted 24 April 1996



ELSEVIER

Fonds Documentaire ORSTOM



010013551

Fonds Documentaire ORSTOM

Cote: B*13551 Ex: 1

GEODERMA

AN INTERNATIONAL JOURNAL OF SOIL SCIENCE

EDITORS-IN-CHIEF

A.B. McBratney, Sydney, N.S.W.
K. McSweeney, Madison, Wisc.
D.L. Sparks, Newark, Del.

HONORARY EDITOR

R.W. Simonson, Oberlin, Ohio

EDITORIAL BOARD

G.H. Bolt, Wageningen	M. Robert, Versailles
J. Bouma, Wageningen	M. Schnitzer, Ottawa, Ont.
R.J. Coventry, Townsville, Qld.	U. Schwertmann, Freising
K. Dalsgaard, Arhus	N. Senesi, Bari
R.B. Daniels, Raleigh, N.C.	S. Shoji, Sendai
F. de Coninck, Ghent	G. Sposito, Berkeley, Calif.
J. de Gruijter, Wageningen	K. Stahr, Stuttgart
J.M. de Villiers, Pietermaritzburg	G. Stoops, Ghent
D. Dent, Norwich	L. Stroosnijder, Wageningen
D.P. Franzmeier, West Lafayette, Ind.	R.S. Swift, Glen Osmond, S.A.
K. Haider, Deisenhofen	P.B. Tinker, Oxford
R. Horn, Kiel	G.C. Topp, Ottawa, Ont.
P.M. Huang, Saskatoon, Sask.	N. van Breemen, Wageningen
R.F. Isbell, Townsville, Qld.	E. van Ranst, Ghent
H.E. Jensen, Copenhagen	A. van Wambeke, Ithaca, N.Y.
E.F. Kelly, Fort Collins, Colo.	Gy. Várallyay, Budapest
K. Kyuma, Hikone	M.J. Vepraskas, Raleigh, N.C.
W.L. Lindsay, Fort Collins, Colo.	H. Vereecken, Jülich
A.R. Mosier, Fort Collins, Colo.	R.J. Wagenet, Ithaca, N.Y.
M. Oades, Glen Osmond, S.A.	G.J. Wall, Guelph
Ya.A. Pachepsky, Moscow	A.W. Warrick, Tucson, Ariz.
R.L. Parfitt, Palmerston North	D.H. Yaalon, Jerusalem

Scope of the journal

The primary intention of the journal is to stimulate wide interdisciplinary cooperation and understanding among workers in the different fields of pedology. Therefore, the journal tries to bring together papers from the entire field of soil research, rather than to emphasize any one subdiscipline. Interdisciplinary work should preferably be focused on occurrence and dynamic characterization in space and time of soils in the field.

Publication Information

Geoderma (ISSN 0016-7061). For 1996 volumes 69–74 are scheduled for publication. Subscription prices are available upon request from the publisher. Subscriptions are accepted on a prepaid basis only and are entered on a calendar year basis. Issues are sent by surface mail except to the following countries where air delivery via SAL is ensured: Argentina, Australia, Brazil, Canada, Hong Kong, India, Israel, Japan, Malaysia, Mexico, New Zealand, Pakistan, PR China, Singapore, South Africa, South Korea, Taiwan, Thailand, USA. For all other countries airmail rates are available upon request. Claims for missing issues must be made within six months of our publication (mailing) date. Please address all your requests regarding orders and subscription queries to: Elsevier Science B.V., Customer Support Department, P.O. Box 211, 1000 AE Amsterdam, The Netherlands. Fax: +31-20-4853432.

US mailing notice – *Geoderma* (ISSN 0016-7061) is published monthly by Elsevier Science B.V. (Molenwerf 1, Postbus 211, 1000 AE Amsterdam). Annual subscription price in the USA US\$ 1482 (US\$ valid in North, Central and South America), including air speed delivery. Application to mail at periodicals postage rate is pending at Jamaica, NY 11431.

USA POSTMASTERS: Send address changes to *Geoderma*, Publications Expediting, Inc., 200 Meacham Avenue, Elmont, NY 11003.

Airfreight and mailing in the USA by Publications Expediting.

Advertising information:

Advertising orders and enquiries may be sent to: *International*: Elsevier Science, Advertising Department, The Boulevard, Langford Lane, Kidlington, Oxford, OX5 1GB, UK; Tel.: (+44) (0) 1865 843565; Fax: (+44) (0) 1865 843976. *USA and Canada*: Weston Media Associates, Dan Lipner, P.O. Box 1110, Green Farms, CT 06436-1110, USA; Tel.: +1 (203) 261 2500; Fax: +1 (203) 261 0101. *Japan*: Elsevier Science Japan, Marketing Services, 1-9-15 Higashi-Azabu, Minato-ku, Tokyo 106, Japan; Tel.: +81 3 5561 5033; Fax: +81 3 5561 5047.

Petrological differentiation patterns and geomorphic distribution of ferricretes in Central Africa

Anicet Beauvais^{a,*}, Claude Roquin^b

^a *Institut Français de Recherche Scientifique pour le Développement en Coopération (ORSTOM), UR12-TOA, 32 Avenue Henri Varagnat, 93143 Bondy Cedex, France*

^b *Centre de Géochimie de la Surface, UPR 6251 C.N.R.S, Institut de Géologie, 1, rue Blessig, 67084 Strasbourg Cedex, France*

Received 24 May 1995; accepted 24 April 1996

Abstract

Geomorphic distribution and petrological differentiation patterns of ferricretes widespread on landsurfaces were studied in the Dembia–Zemio area, southeastern Central African Republic. Four types of ferricretes are distributed on high plateaux, hillslopes and low plateaux. The main contrast corresponds to the differentiation between ferricretes of high plateaux rich in poorly hydrated minerals, hematite and kaolinite, and those covering hillslopes and low plateaux richer in hydrated minerals, goethite and gibbsite. A Principal Component Analysis of geochemical and mineralogical data was used to characterize the main differentiation patterns of ferricretes in relation with their petrographic facies and the geomorphic features of the landscape. The distribution of secondary minerals and their relationships to trace elements within and between the ferricrete types reflects differences in weathering and erosion processes. Our results document that the petrological patterns and the distribution of ferricretes are related to geomorphic features depending on hydroclimatic variations that govern the landscape evolution of many tropical shields.

Keywords: ferricrete; Central Africa ; petrology; geochemistry; geomorphology

1. Introduction

In southeastern Central African Republic, the bedrock is deeply weathered and uniformly covered by thick ferricretes. The weathering profiles developing from different parent rocks always exhibit the following upward succession of layers: saprolite, mottled clay and ferricrete (Tardy and Nahon, 1985; Nahon, 1986). The geochemical

* Corresponding author. E-mail: beauvais@bondy.orstom.fr

processes involved in the weathering profile development imply complete leaching of alkalis and earth-alkalis, partial desilication from the parent-rock minerals, and thus, relative accumulations of iron and aluminium (Delvigne, 1965; Tardy, 1969; Millot, 1970; Nahon, 1991). In contrast, the minor transition elements are generally trapped in the secondary Al- and Fe-oxihydroxides and clay minerals (Trescases, 1975; Schwertmann and Taylor, 1977; Mosser, 1980), which are, in turn, the main components of ferricretes (Nahon, 1976; Leprun, 1979; Tardy and Nahon, 1985; Tardy et al., 1988a). Under tropical climates with a pronounced dry season, bio-physical processes are often involved in the reworking of weathering profiles, implying either the dispersion of the heavy minerals and relict quartz onto the landsurface, or the vertical translocation through the macropores of weathering profiles (Brimhall and Dietrich, 1987; Butt and Zeegers, 1989; Freyssinet et al., 1989; Freyssinet, 1990; Lecomte and Colin, 1989; Colin and Vieillard, 1991; Colin et al., 1992). Geochemical and mineral prospecting in lateritic environments requires knowledge of the nature, the distribution and the geochemical patterns of lateritic formations concealing the parent rocks (Nalovic, 1977; Davies and Bloxham, 1979; Zeegers and Leprun, 1979; Matheis, 1981; Matheis and Pearson, 1982; Butt, 1987; Butt and Zeegers, 1989; Roquin et al., 1989; Boski and Herbosch, 1990).

Many studies have addressed the influence of parent rocks on the petrological differentiation patterns of vertical weathering profiles capped with old pedogenic ferricretes (Leprun, 1979; Zeegers and Leprun, 1979; Matheis, 1981; Ambrosi and Nahon, 1986; Nahon, 1991), but the processes governing the spatial distribution of ferricretes onto landsurfaces were rarely investigated (Butt and Zeegers, 1989; Roquin et al., 1989). However, more attention has been paid recently to the regional distribution of ferricretes tempering their effective relationships to parent rock variations and inferring that their mineralogical variation patterns over the world might be considered as reflecting climatic changes driven by continental plate drift (Tardy et al., 1988b, 1991). Although the saprolite and the mottled clay layers of weathering profiles often relate to the parent-rock geochemistry (Ambrosi and Nahon, 1986; Nahon, 1991; Tardy, 1993), the ferricretes can lose this geochemical inheritance under the influence of environmental factors governing landscape evolution (Boeglin and Mazaltarim, 1989; Tardy et al., 1988a). Considering that the bedrock of our study area is composed of undifferentiated basic metamorphic rocks (Mestraud, 1982; Beauvais, 1991), we explore the relations between the ferricrete petrological differentiation patterns and their geomorphic distribution in the landscape.

2. Geographic features of the study area

The study area of 260 km² around the village of Guénékoumba between Dembia and Zemio (Figs. 1 and 2) forms part of the African shield, thought to have been tectonically stable for 70 My (Boulvert, 1996). This area is included in a wider geomorphic region of 3000 km² known as "Haut-Mbomou plateau" which was investigated for geological mapping and base metal prospection (Mestraud, 1982). The Haut-Mbomou plateau is extensively covered by ferricretes and the geological substratum corresponds to a large complex of basic rocks, named Complex of Mbomou and composed of metamorphic

volcano-sedimentary formations corresponding to amphibolite and green-schist facies crossed by elongated granitic intrusions and dykes of dolerites in the southwestern area of the Haut-Mbomou plateau (Mestraud, 1982). Although the extensive lateritic cover masks the parent rocks in our field area, some fresh rocks collected at the surface of plateaux and hillslopes are amphibole schists. Similar rocks were also identified in some deeply incised thalwegs. Hence, we consider these amphibole schists as the parent rocks in our study area.

This region has a tropical humid climate characterized by (1) a short dry season from December to February, a long wet season from May to October, and 3 months of interseason, in November, March and April; (2) a mean annual rainfall of 1600 mm; (3) a mean annual temperature of 25°C; and (4) a mean annual relative humidity of 80% ranging from 50% to 95% (Boulvert, 1986; Franquin et al., 1988; Beauvais, 1991). The vegetation cover consists of a semi-humid forested savanna. Large stretches of grass and bare lands alternate on the plateaux and hillslopes, while a dense humid forest occupies the valleys and the high plateau edges (Fig. 2).

Three main landform units were distinguished in the study area: high plateaux, hillslopes and low plateaux (Fig. 2). All three are armoured by 3 to 5 metres of ferricretes capping lateritic weathering profiles exhibiting thicknesses of several tens of metres (Beauvais, 1991). These geomorphic units are representative of the Haut-Mbomou plateau extending on several square kilometres. There is no evidence in the field to relate the geomorphic patterns to differentiation of the geological basement. The high plateaux as a whole form a regional warped erosion surface with many points culminating at 650 m above sea level (a.s.l.). This landsurface envelope gently slopes down (0.1 to 0.2%) towards the main hydrographic channels, the Ouara river to the West and the Mbomou river to the South. Individual high plateaux are limited by an erosion scarp of one metre height, and surrounded with a ring of dense semi-humid forest. Further downslope, another metric scarp separates the forested hillslope from the bare hillslope. The high plateau landsurface is globally planconvex with some concave area, while the

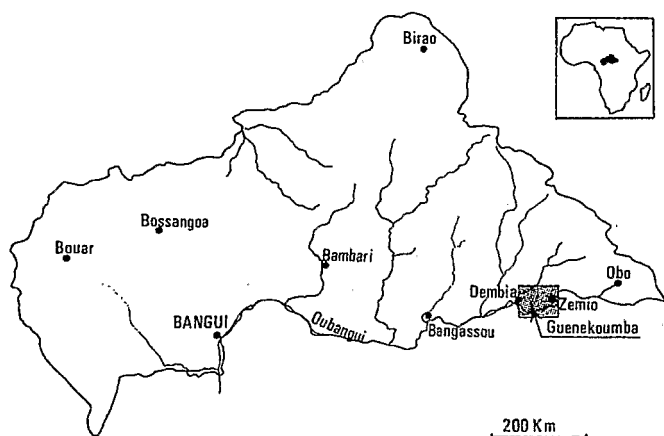


Fig. 1. Location of the study area in Central African Republic.

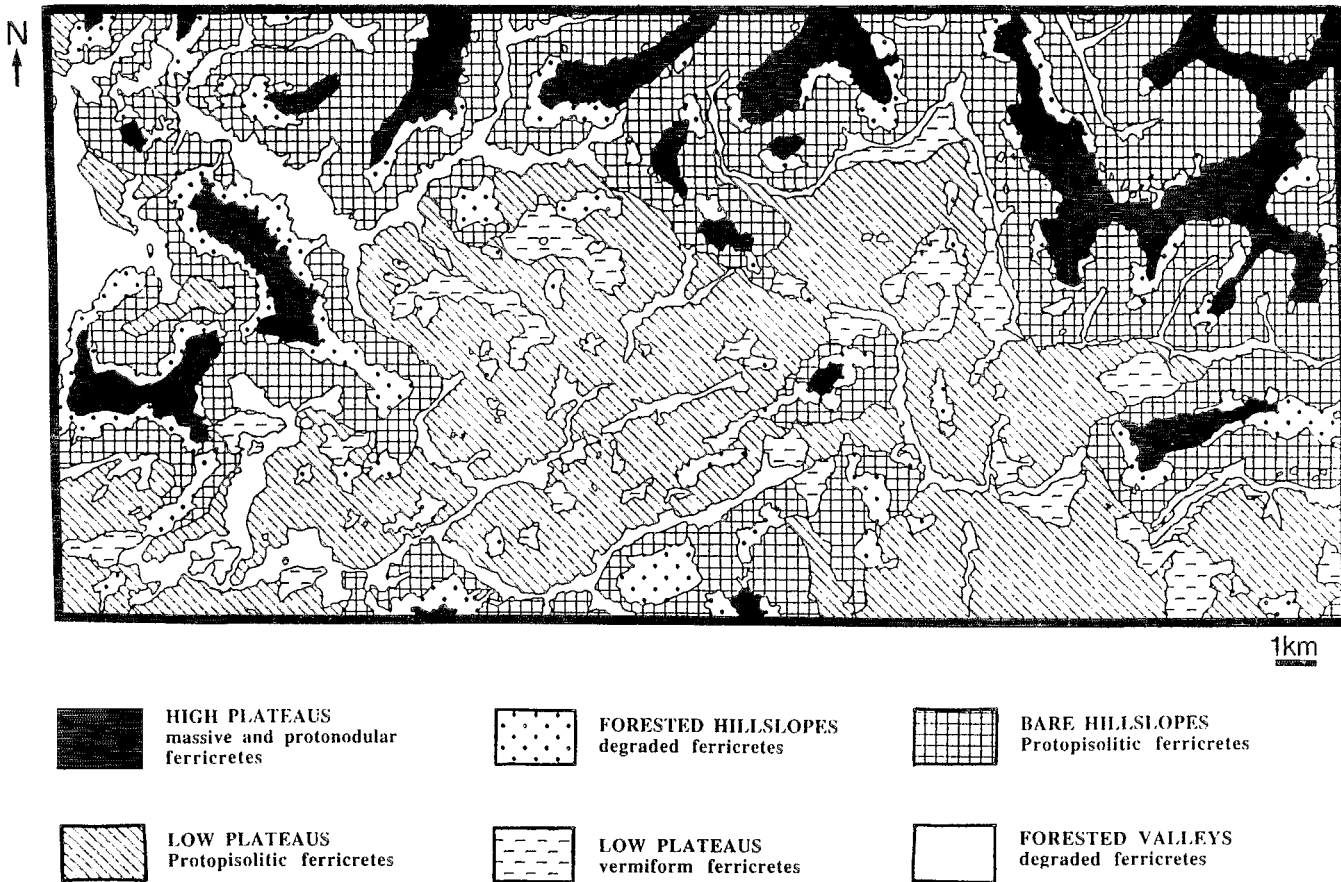


Fig. 2. Geomorphological map and spatial distribution of ferricrete facies.

hillslopes present straight and concave profiles with gradients ranging from 5% on the bare hillslope to 10% on the forested hillslope. In contrast, the low plateaux are planconcave and they are always separated from high plateaux by a thalweg or a hillslope (Fig. 2). Hillslope and low plateau landsurfaces are densely covered by termitaria (i.e., 1 per square metre, on average), whose the soft clayey–silty material is dispersed downslope by overland flow. During the rainy season, “swampy” area take place on concave surfaces by subsurface saturation flow.

3. Methods

The mapping of geomorphic units and associated lateritic formations was first realized at a 1:50 000 scale from field and aerial photograph observations (Boulvert, 1976; Beauvais, 1991). The lateritic landsurface was then investigated and ferricretes were sampled to characterize their petrological differentiation patterns. Petrographic facies, mineralogical and chemical compositions were analysed for 204 samples and compared to the geomorphic, hydrologic and phytogeographic characteristics recorded at each sampling site. Ferricrete blocks of at least 1000 cm³ were regularly collected on each landform unit at a depth ranging from 10 cm to 50 cm. Petrographic facies were described from macroscopic and microscopic observations. Each sample was then crushed to 5 mm and sorted to produce 100 g of powder with a sieve size ranging from 64 to 120 μm for chemical and mineralogical analysis.

Major element contents analysed by spark emission spectrometry (SiO₂, Al₂O₃, Fe₂O₃, MgO, CaO, P₂O₅, TiO₂) and by flame emission spectrometry (Na₂O, K₂O) are given in oxide percent. Trace elements analysed by plasma emission spectrometry ICP (Sr, Ba, V, Ni, Co, Cr, Cu, Zn, Sc, Y, Zr, Mn, La, Yb, and Nb) are given in ppm. Samples were dried prior to the analysis and weight loss on ignition (LOI) was measured after a 1000°C calcination. Elements with concentrations systematically below detection limits (d.l.) were neglected. Those are MgO (d.l. = 0.02%), CaO (d.l. = 0.20%), Na₂O and K₂O (d.l. = 0.01%), Eu (d.l. = 10 ppm) and Lu (d.l. = 1 ppm).

The mineralogical analyses were obtained from X-ray diffraction (XRD) of unoriented powder preparations. Mineral contents were estimated measuring characteristic intensity of X-ray peak weighted by a calibration coefficient defined for each mineral, employing normative calculations (Mazaltarim, 1989). The error in estimation ranges from 1 to 3%. Therefore, each sample was defined by seven mineralogical variables, corresponding to the estimated contents of kaolinite (Kaol), quartz (Quar), gibbsite (Gib), goethite (Goet), hematite (Hema), and the ratios, RHG equal to 100*hematite/(goethite + hematite), and RKGi equal to 100*kaolinite/(gibbsite + kaolinite).

The differentiation patterns for the whole set of ferricrete samples were defined applying a Principal Component Analysis (PCA) to geochemical and mineralogical data (SAS, 1985). This statistical procedure is based on the determination of eigenvectors with their associated eigenvalues from the correlation matrix, followed here by an application of the varimax rotation procedure (Lebart et al., 1979). The main differentiation trends in the data set are expressed by the first factors (i.e., the principal

components) which are new independent synthetic variables characterized by their association with some elements and/or minerals, as it was successfully applied to soils and weathering system studies (Litaor et al., 1989; Boski and Herbosch, 1990; Roquin et al., 1990; Donkin and Fey, 1991). Within each factor, for each element and mineral, the correlation loadings ranging from -0.4 to 0.4 were considered as non-significant. A representation of samples on factor score diagrams illustrates the ferricretes differentiation patterns within and between morpho-petrological categories identified in the field.

4. Field characteristics of ferricretes

4.1. Description of ferricretes

Four ferricrete facies were identified based on both macroscopic descriptions (Fig. 3), according to the typologic nomenclature recently proposed by Tardy (1993), and on previous microscopic observations (Beauvais, 1991; Beauvais and Colin, 1993).

(a) The massive ferricretes exhibit an indurated compact hematitic matrix purple-reddish coloured, with a fine porosity but without nodules or obviously defined geometric elements (Fig. 3a).

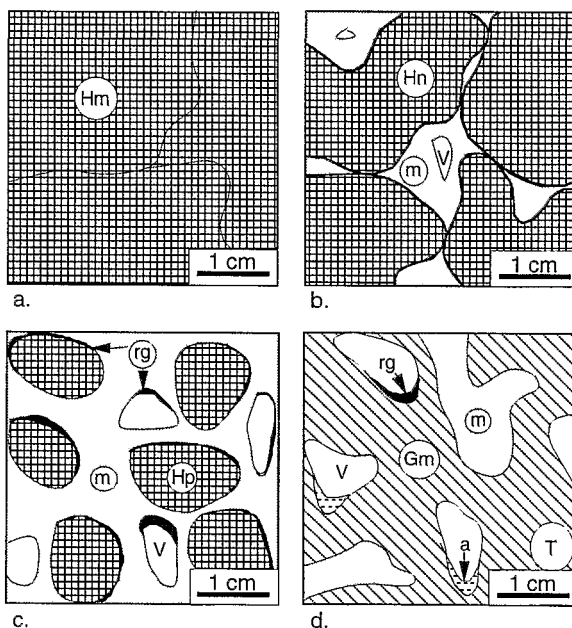


Fig. 3. Petrographical sketches of the four ferricrete facies sampled on the landsurface. (a) massive; (b) protonodular; (c) protopisolithic; (d) vermiform. (Hm = Hematitic matrix; Hn = hematitic nodular domain; m = clayey ferruginous matrix; V = vacuole; Hp = Hematitic protopisolite; rg = goethitic rim; Gm = goethitic matrix; a = argilan; T = tubule.)

(b) The protonodular ferricretes show large coalescent purple-reddish hematitic nodular domains (> 1 cm), coexisting with a slightly indurated clayey–ferruginous matrix crossed by small vacuoles (< 1 cm) (Fig. 3b). This facies may also exhibit small goethitic rims around the hematitic domains, and also some gibbsite scattered within the matrix. In both (a) and (b) facies, the ferruginous matrix is rich in hematite and kaolinite booklets of 100–200 μm in length, deriving from pseudomorphic weathering of micas, feldspars and amphiboles.

(c) The protopisolitic ferricretes generally present purple-reddish hematitic protopisolites outlined by peripheral goethitic rims and cortex. The protopisolites have sizes approximating 1 cm and they are enclosed within a red-yellowish clayey–ferruginous matrix crossed by cm-sized vacuoles (Fig. 3c). Microscopic observations revealed the development of secondary gibbsite through the matrix and within the vacuoles. Also, we have observed some relics of ilmenite showing partial dissolution features.

(d) The vermiform ferricrete is essentially characterized by a yellow–brown matrix composed of microcrystalline mixture of kaolinite and goethite, with a few centimetre-length diffuse hematitic domains and some relics of quartz. The ferruginous matrix is intersected by a dense network of centimetric vacuoles and tubules, which are often filled with a white fine clayey matrix, and outlined by argillans and brown goethitic rims (Fig. 3d). To a lesser extent, manganeseiferous concretions mainly composed of lithiophorite were also identified in facies (c) and (d), and some relics of micas or feldspars were observed under the microscope in facies (b), (c) and (d), although these minerals were never detected from XRD analyses.

4.2. Regional distribution of ferricretes

The regional distribution of ferricretes is shown on the morphopetrographic map (Fig. 2). About 80% of the total field mapped landsurface (TFML) is covered by ferricretes, while the remaining 20% correspond to forested areas wherein the ferricretes are degraded (Beauvais and Tardy, 1993). Four ferricrete facies, massive, protonodular, protopisolitic and vermiform were differentiated by their petrographic features, and by their location in the landscape. 31 samples of massive and 29 samples of protonodular ferricretes were collected on high plateaux representing 10.5% of TFML; 52 samples of protopisolitic ferricretes were collected on the hillslopes occupying 32% of TFML; 64 samples of protopisolitic ferricretes were sampled on the low plateaux representing 31% of TFML; 28 samples of vermiform ferricretes outcrop on the low plateaux occupying 6.5% of TFML. The protopisolitic ferricretes are widespread on the hillslopes and on the low plateaux, representing 61% of the sampling set. The massive and the protonodular ferricretes are the only two facies covering the surface of the high plateaux and they represent 26% of the sampling. The protopisolitic ferricrete layer of hillslopes may comprise blocks of massive ferricrete with decimetric sizes that exhibit a peripheral brown cortex of goethite. The vermiform ferricretes only outcrop on the low plateaux, and represent 13% of the sampling. This facies is also well developed within the weathering profiles of the hillslopes and low plateaux capped by a protopisolitic ferricrete (Beauvais, 1991; Beauvais and Colin, 1993).

5. Analytical results

5.1. Petrological patterns of ferricretes

The mean and standard deviation values of elements and minerals for the four main petrographic facies distributed on the three geomorphic units are presented in Table 1. At first glance, the mean geochemical compositions indicate that the contents of transition elements versus earth alkalis and rare earth elements do not permit to

Table 1

Comparison of mean chemical and mineralogical compositions of ferricretes according to their petrographic facies and geomorphic location (n = number of samples; M = massive; PN = protonodular; PP = protopisolitic; V = vermiform; m = mean; s = standard deviation; LOI = lost on ignition (1000°C); RHG = 100*hematite/hematite + goethite; RKGi = 100*kaolinite/kaolinite + gibbsite)

Location:	High plateaux				Hillslopes				Low plateaux			
facies:	M		PN		PP		PP		V			
n:	31		29		52		64		28			
	m	s	m	s	m	s	m	s	m	s		
SiO ₂ (%)	15.2	3.4	11.7	2.9	10.9	2.6	10.6	3.3	15.3	3.5		
Al ₂ O ₃	16.3	2.8	15.8	2.0	16.6	2.9	17.2	2.4	17.6	3.1		
Fe ₂ O ₃	57.2	6.3	61.2	4.9	59.7	4.5	58.4	4.9	52.6	6.9		
TiO ₂	1.7	0.3	1.6	0.3	1.4	0.3	1.3	0.3	1.4	0.4		
P ₂ O ₅	0.39	0.14	0.4	0.1	0.5	0.2	0.4	0.1	0.37	0.16		
LOI	8.8	1.5	9.0	1.1	10.6	1.8	11.4	1.6	12.4	0.7		
Sr (ppm)	54	49	30	25	24	26	13	16	12	8		
Ba	47	36	28	19	93	239	54	138	39	57		
V	1372	423	1469	286	1412	363	1325	306	1201	330		
Mn	211	163	222	106	683	1169	612	1132	376	521		
Ni	40	7	43	9	59	30	58	29	61	37		
Co	15	5	14	4	27	17	18	10	19	17		
Cr	330	212	555	187	467	243	609	214	372	159		
Zn	52	21	59	20	74	49	82	41	101	51		
Cu	100	44	95	33	193	173	274	178	528	264		
Sc	46	12	47	12	50	18	62	18	73	18		
Y	9	3	8	2	11	5	12	4	13	4		
Zr	309	70	299	68	278	80	282	67	271	121		
La	52	32	30	17	27	30	20	18	20	10		
Ce	72	45	53	35	101	161	127	171	87	119		
Yb	1.6	0.5	1.4	0.4	1.8	0.7	1.4	1	2.1	1		
Nb	16	4	18	4	16	5	17	5	15	5		
Quartz (%)	1	1	1	1	3	4	3	3	3	2		
Kaolinite	35	9	28	9	23	10	20	7	26	8		
Hematite	48	10	51	10	34	14	28	12	10	7		
Goethite	12	8	13	5	30	18	36	13	58	13		
Gibbsite	5	5	7	5	10	8	12	7	3	5		
RHG	81	11	80	8	54	22	44	19	15	12		
RKGi	90	10	81	12	71	22	63	19	91	12		

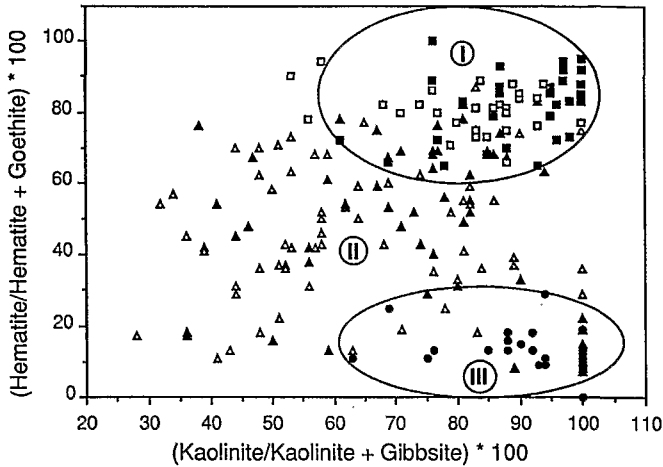


Fig. 4. Mineralogical variation pattern of ferricrete facies according to their geomorphological location (■ massive and □ protonodular of high plateaux; protopisolitic of ▲ hillslopes and △ low plateaux; ● vermiform of low plateaux).

distinguish different parent rocks for the different ferricrete facies. From the high plateaux to the low plateaux, the kaolinite and hematite contents progressively decrease while the goethite content increases with the highest value in the vermiform facies. The protopisolitic ferricretes exhibit the highest gibbsite content. The variations of ferricrete mineralogical composition are represented in a rectangular diagram, RHG versus RKGi (Fig. 4). The vermiform facies of low plateaux is relatively rich in goethite and poor in hematite and clearly separated from the massive and protonodular facies of high plateaux, which are defined by higher contents of hematite. Both are relatively high in kaolinite. Samples of protopisolitic facies of hillslopes and low plateaux present a wide range of composition between the ferricretes of high plateaux and the vermiform facies of low plateaux.

The mineralogical variations were also analysed by examining the moving average of each mineral abundance for classes of 5% Fe_2O_3 and Al_2O_3 with a re-covering step of 2.5%, i.e. for Fe_2O_3 amounts ranging from 40% to 45%, then from 42.5% to 47.5% and so forth... (Figs. 5 and 6). Three main trends are evidenced on these diagrams, justifying the distinction of three ferricrete categories, that is consistent with the differentiation patterns yielded by the Fig. 4.

The first category (I) corresponds to the massive and protonodular ferricretes of high plateaux which are, on the average, the richest in hematite and kaolinite, and the poorest in goethite (Table 1 and Fig. 4). When the iron content increases and the alumina decreases, the hematite content increases, the kaolinite and gibbsite contents decrease while quartz and goethite remain roughly constant (Figs. 5 and 6). For the two facies of high plateaux, the evolution curves of gibbsite and kaolinite versus Al_2O_3 are not parallel, an increase in Al_2O_3 for the massive ferricretes corresponding to an increase in gibbsite rather than in kaolinite (Fig. 6).

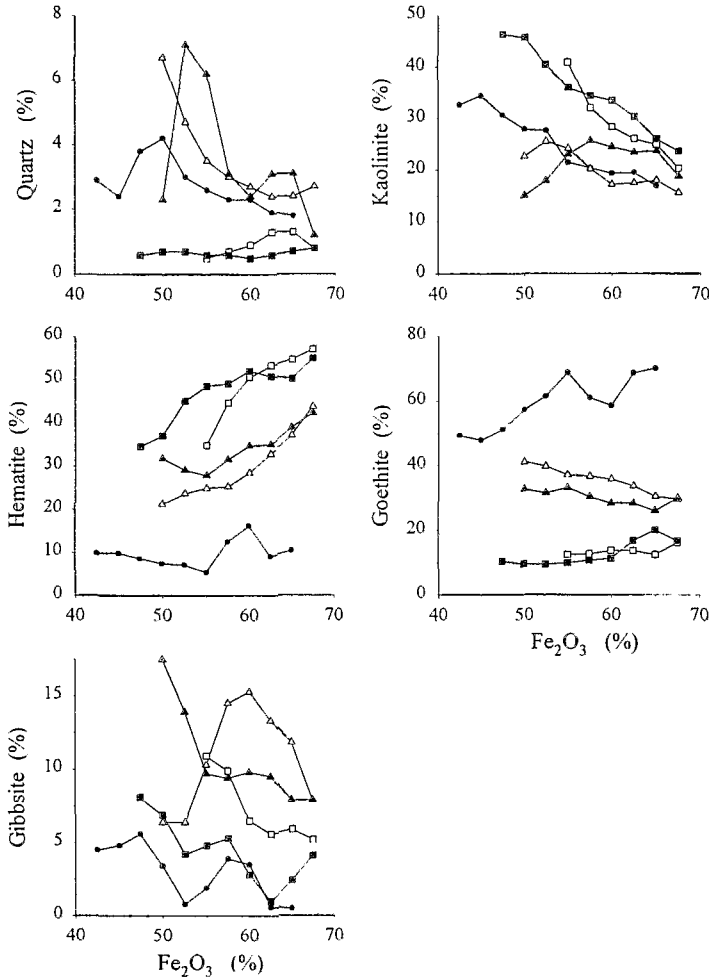


Fig. 5. Variation of mineral contents as a function of iron moving average calculated for classes of 5% Fe₂O₃. For symbols see Fig. 4.

The second category (II) is composed of protopisolithic ferricretes of hillslopes and low plateaux that are less hematitic but more goethitic. This facies presents the highest gibbsite contents, and also some quartz (Table 1 and Figs. 5 and 6). For these ferricretes, an increase in iron content is related to hematite rather than to goethite (Fig. 5), while an increase in aluminium content reflects an enrichment in gibbsite rather than in kaolinite (Fig. 6). Although the mineralogical evolution curves of the protopisolithic facies of hillslopes and low plateaux are very similar, the ferricretes of low plateaux are slightly richer in goethite and gibbsite and poorer in hematite and kaolinite than those of hillslopes (Table 1 and Fig. 6).

The third category (III), corresponds to the vermiform ferricretes of low plateaux that are the richest in goethite, the poorest in hematite and the less ferruginous (Table 1). In

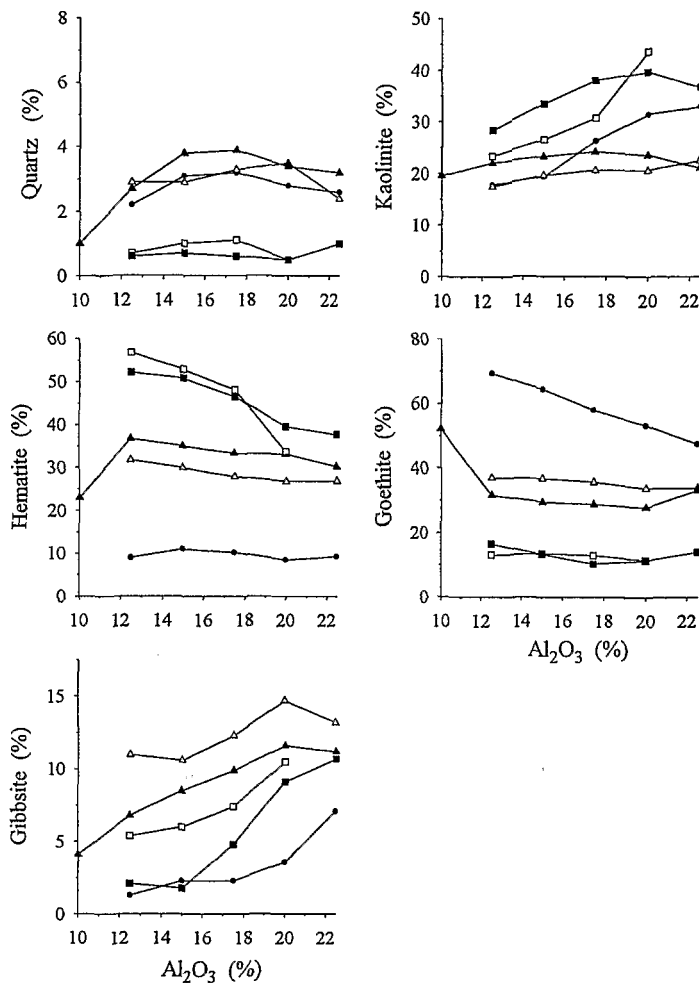


Fig. 6. Variation of mineral contents as a function of aluminium moving average calculated for classes of 5% Al_2O_3 . For symbols see Fig. 4.

contrast with the protopisolithic facies, an increase in iron content and a decrease in alumina are related to an increase in goethite and a loss of kaolinite (Figs. 5 and 6). This ferricrete facies contains small amounts of quartz and gibbsite related to iron and aluminium contents respectively (Figs. 5 and 6).

For the massive and protonodular ferricretes of the high plateaux, iron is mainly related to the hematite content, while for the vermiform facies of low plateaux it is related to the goethite content (Fig. 5). For the protopisolithic ferricrete of hillslopes and low plateaux, the iron content decreases with the transformation of hematite to goethite. In contrast with the other facies, the decrease in iron content for the protopisolithic facies of hillslopes is also related to a loss of kaolinite and a strong increase in gibbsite (Fig. 5).

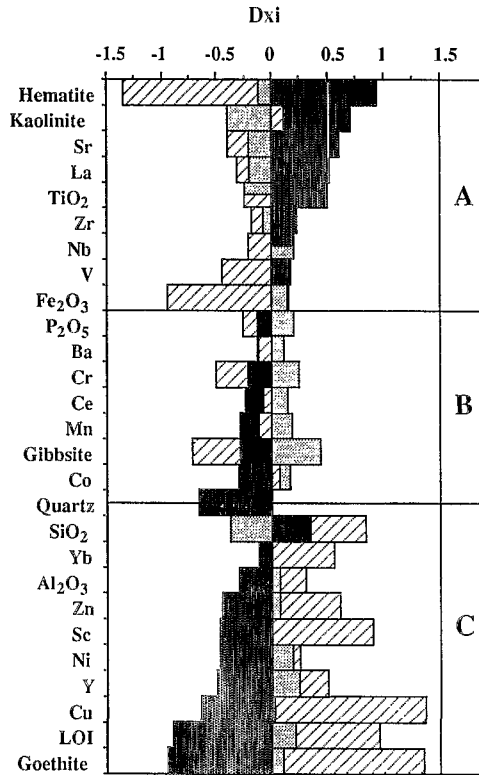


Fig. 7. Mineralogical and geochemical contrast of ferricrete categories according to the background differentiation index (Dx_i) of elements for the three ferricrete categories (LOI = loss on ignition; black: massive + protonodular facies of high plateaux; shaded: protopisolithic facies of hillslopes and low plateaux; hatched: vermiform facies of low plateaux; A, B and C represent the three groups of elements whose Dx_i is maximum in one of the three categories).

5.2. Geochemical differentiation contrasts between the ferricretes

A more synthetic analysis of petrological differentiation contrasts is given in Fig. 7 for the three categories of ferricretes described above: (I) massive and protonodular ferricretes of high plateaux; (II) protopisolithic ferricretes of hillslopes and low plateaux; and (III) vermiform ferricretes of low plateaux. A differentiation contrast index Dx_i for each chemical and mineral element x was calculated as the standardized deviation of within-group mean for each ferricrete sample category i such that:

$$Dx_i = (\text{mean}(x)_i - m(x)) / s(x) \quad (1)$$

where $m(x)$ and $s(x)$ respectively represent the overall mean and standard deviation of element x for the whole sample set. A negative or positive value of Dx_i indicates the depletion or the enrichment contrast of element x relative to the overall mean of this element within a sample category i expressed in unit of standard deviation. The

elements were first ranked according to the decreasing contrast value Dx_i for the high plateau ferricrete samples, and then allocated to one of the three ferricrete categories according to their higher Dx_i in each category (Fig. 7). The first group of elements (A) is composed of Sr, TiO_2 , La, V, and also Zr and Nb, associated to hematite and kaolinite, which exhibit higher positive Dx_i in the ferricretes of high plateaux. In contrast, these elements have negative Dx_i in the vermiform ferricretes of low plateaux, except for kaolinite. They also tend to be more depleted in the protopisolithic facies. The second group of elements (B) is characterized by higher contents of gibbsite in the protopisolithic facies contrasting with lower content of kaolinite (Fig. 7). The development of Mn- oxy-hydroxides in this facies is reflected by highest positive Dx_i for Mn and associated elements, Ba, Ce, and Co. A relative enrichment of P_2O_5 and Cr can also be noticed. The third group of elements (C) corresponds to higher contents of SiO_2 , Al_2O_3 , LOI, and also Cu, Y, Sc, Ni, Zn, Yb associated to goethite enrichment characterizing the vermiform ferricretes of the low plateaux. The ferricretes of high plateaux are the richest in poorly hydrated minerals, kaolinite and hematite, as well as in chemical elements with low mobility, except Sr. In contrast, the protopisolithic and vermiform ferricretes of hillslopes and low plateaux are the richest in hydrated minerals, gibbsite and goethite respectively, and they are also the richest in chemical elements which generally present a higher mobility in the lateritic environments (Tardy, 1969; Nalovic, 1977; Davies and Bloxham, 1979; Matheis, 1981; Roquin et al., 1989).

5.3. Principal component analysis

The principal component analysis (PCA) applied to the whole data set yields six independent factors explaining 70.1% of the total variance (Table 2). Comparison of results of the Table 2 and Fig. 7 allows to interpret each factor. The first factor contributing to 29.5% of the explained variance is positively loaded with the goethite correlated to LOI and trace elements Cu, Sc, Zn, Ni, Y and Yb and negatively loaded

Table 2

Correlation of chemical elements and minerals with each factorial axis defined by the Principal Component Analysis (LOI = loss on ignition; loading values are given in parentheses)

Factorial axis	% explained variance	Positive loadings	Negative loadings
F1	29.5	LOI (0.76), Ni (0.56), Zn (0.68), Cu (0.88), Y (0.74), Sc (0.74), Yb (0.5), Goethite (0.86)	Hematite (0.82)
F2	17.5	SiO_2 (0.69), Al_2O_3 (0.81), Zr (0.47), Kaolinite (0.46)	Fe_2O_3 (0.93)
F3	12.2	Cr (0.77), Gibbsite (0.7)	SiO_2 (0.51), Kaolinite (0.46)
F4	15.5	Mn (0.93), Ba (0.88), Co (0.65), Ce (0.69)	
F5	12.8	TiO_2 (0.45), P_2O_5 (0.54), Zr (0.58), Nb (0.75), Quartz (0.48)	
F6	12.5	Sr (0.84), La (0.83), V (0.43)	

with hematite, reflecting the patterns of vermiform facies. The correlation matrix indicates that LOI is correlated to each trace element. This factor opposes ferricretes of high plateaux to the other ferricretes. Factor 2 contributing to 17.5% of the explained variance separates a group composed of Al_2O_3 , SiO_2 and kaolinite with Zr exhibiting positive loadings, from Fe_2O_3 with a negative loading. This factor accounts on the undifferentiated ferruginization process of clayey matrices in all ferricrete facies, and also the Al-substitution in Fe-oxihydroxides (Beauvais, 1991). Factor 3 representing 12.2% of the explained variance opposes positive loadings on gibbsite and Cr to negative loadings on kaolinite and SiO_2 reflecting the contrast between gibbsite and kaolinite formation processes in the protopisolithic facies. Examination of the correlation shows that gibbsite is relatively correlated to LOI ($r = 0.31$). Factor 4 contributing to 15.5% of the explained variance shows high positive loadings on Mn, Ba, Ce and Co, describing the secondary development of Mn-oxhydroxides, effective in protopisolithic and vermiform facies. The analysis of correlations reveals two distinct trends separated by a threshold in Mn-content. When Mn-content is lower than 800 ppm, intercorrelations between Mn, Ba, Co and Ce do not exist, and positive correlations appear between Sr, Ba, La and Ce, while the global relationship revealed by the factor 4 is only effective when Mn-content is higher than 800 ppm. Factor 5 representing 12.8% of the explained variance express the geochemical patterns of residual heavy minerals as shown by the positive loadings on TiO_2 , P_2O_5 , Zr and Nb with quartz, while Factor 6 contributing to 12.5% of the explained variance exhibits positive loadings on Sr, La and V (Table 2),

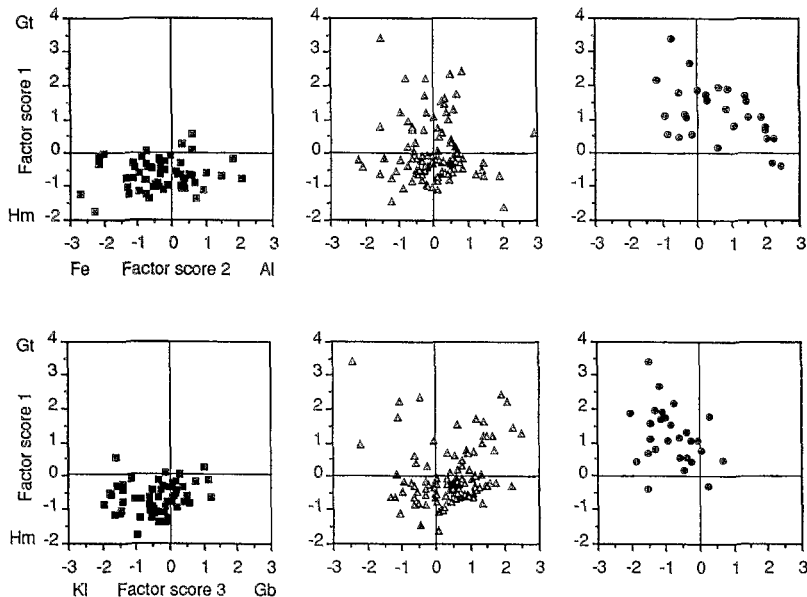


Fig. 8. Petrological differentiation pattern of ferricrete categories reflected by (a) the first factor score diagram F1 vs. F2, and (b) the second factor score diagram. F1 vs. F3 (■ massive and protonodular facies of high plateaux; △ protopisolithic facies of hillslopes and low plateaux; ● vermiform facies of low plateaux; Gt = Goethite; Hm = Hematite; Kl = Kaolinite; Gb = Gibbsite).

that reflects higher abundance of relics of feldspars and micas. The first four factors contributing to 74.7% of the explained variance are loaded by chemical elements showing relationships with minerals depending on lateritic weathering processes, while both factors 5 and 6 representing 25.3% of the explained variance are loaded by chemical elements with no clear affinities to the lateritic mineral phases. These two factors may account on some parent rock inheritance which is better expressed in ferricretes of high plateaux than in those of hillslopes and low plateaux (Fig. 7).

The projections of ferricrete samples on the factor diagrams F1 versus F2 and F1 versus F3 show the main differentiation trends within and between the ferricrete categories (Fig. 8). Three distinct petrological paths are expressed by the factorial axes corresponding to the contrasts goethite/hematite, alumina/iron oxide, and gibbsite/kaolinite. The first diagram of factor scores, F1 versus F2, highlights differences in ferruginization processes discriminating the hematitic ferricretes of high plateaux from the vermiform facies of low plateaux which exhibit another trend between two end-members, ferruginous-goethitic and aluminous-kaolinitic (Fig. 8a). This also may account on the development of goethitic rims and cortex in kaolinitic matrix of vermiform facies as well as around hematitic nodules of protopisolic facies. The second diagram of factor scores, F1 versus F3, confirms the results of the Fig. 4, showing different contrasts between the petrological differentiation patterns of the three ferricrete categories. The ferricretes of high plateaux are represented by an hematite–kaolinite pattern, while the protopisolic and vermiform ferricretes of hillslopes and low plateaux are mainly characterized by a goethite–gibbsite and a goethite–kaolinite pattern respectively (Fig. 8b). In both factorial diagrams, the protopisolic ferricrete facies define a wide domain ranging from the ferricretes of high plateaux to the vermiform ferricretes of low plateaux.

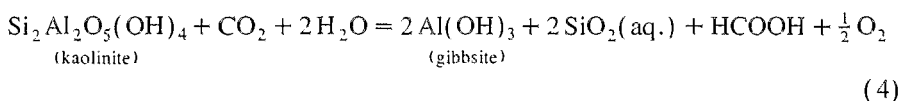
6. Discussion

Our results document that the differentiation patterns and distribution of ferricretes in the Haut-Mbomou region may be governed by interactions between geomorphic and hydroclimatic processes, once the weathering profiles are sufficiently developed on parent amphibole schists. Although less advanced stages of weathering strongly depend on parent rock type (Leprun, 1979; Zeegers and Leprun, 1979; Matheis, 1981; Ambrosi and Nahon, 1986; Nahon, 1991; Tardy, 1993), the influence of hypothetical lithologic variations on relatively old ferricretes is unlikely in our study area. It has been shown that the iron-richness and evolution degree (i.e., age) of similar ferricretes of West Africa tended to blur parent rock signatures (Tardy et al., 1988a; Boeglin and Mazaltarim, 1989; Roquin et al., 1990). In our field area, the differentiation patterns of ferricretes follow the geomorphic evolution of landscape depending on climatic variations to humid or to dry tendencies. Climatic factors continuously model the landforms, modifying the slope gradients, the biological patterns and drainage conditions in soil profiles, which, in turn, influence the way the ferricretes evolve. The actual climatic conditions favour the petrological transformations of ferricretes wherever the forest grows and the water is seasonally retained on concave surfaces, inviting to consider the

influence of water activity and organic matter in mineralogical patterns of ferricretes (Tardy and Nahon, 1985; Beauvais and Tardy, 1993; Tardy, 1993). The high plateau ferricretes mainly composed of poorly hydrated minerals, hematite and kaolinite, generally do not show such transformations, except the protonodular exhibiting secondary goethitic rim around hematitic nodules or gibbsite within the ferruginous matrices. In contrast, protopisolithic and vermiform ferricretes richer in hydrated minerals gibbsite and goethite, respectively, exhibit further petrological variations. As a fact, the vestiges of massive hematitic facies within the protopisolithic layers of hillslopes indicate pedogenetic and morphogenetic relations between high plateaux and hillslopes. In this way, the ferricretes of high plateaux are older than the other facies, and their petrological patterns may reflect past hydroclimatic conditions, while the facies of hillslopes and low plateaux exhibit mineralogical patterns related to actual geomorphic and climatic conditions. The transformation of hematite into goethite is conditioned by a dissolution–reprecipitation mechanism (Schwertmann and Taylor, 1977), while the transformation of kaolinite into gibbsite obeys to a desilication mechanism. However, these mechanisms depend on both water activity and partial pressure of carbon dioxide produced by the mineralization of organic matter (Tardy, 1993), such as



So, the transformation of hematite and kaolinite under both hydration and redox process can be described by the following global reactions



Both field observations and results support this model, whose the above equations are likely involved in the differentiation patterns of protopisolithic facies, and to a lesser extent, in protonodular of high plateaux. However, the formation of gibbsite in the both facies is further conditioned by a relatively good drainage on plan surfaces located at the edges of high plateaux, and on hillslopes and low plateaux overhanging the valley heads. The petrological patterns of ferricretes developed on the planconvex surfaces of high plateaux further reveal that dehydration and oxydation processes have characterized the ferruginization of kaolinite booklets, by preserving a residual fraction of heavy minerals containing Ti, Zr and Nb, and silicate minerals bearing Sr, La and V. The petrological patterns of vermiform and protopisolithic facies further suggest that local hydrodynamic conditions relative to concave surfaces of low plateaux and hillslopes periodically liable to floodings may also influence the trace element behaviour. Indeed, those landsurfaces exhibit much more concavities than the high plateaux, and they are also covered by termitaria composed of reworked clayey–silty materials undergone to surface erosion processes.

Previous studies carried out in similar environments of West Africa have shown that the termitaria materials contained quartz and heavy minerals as ilmenite and zircon, and

that they have been likely transported upward by termites through connected macropores from underlying mottled and saprolite layers (Eschenbrenner, 1987; Freyssinet, 1990). The vermiform facies exhibiting such connected macropores are potential places for termite activity. In fact, the development of secondary goethite with Mn, Cu, Ni, Zn, Co, Sc, Y and Yb through illuviated clayey matrices of vermiform facies can be enhanced by the presence of organic matter (Kämpf and Schwertmann, 1983; Boski and Herbosch, 1990) yielding hydromorphic conditions, which prevail on concave surfaces of hillslopes and low plateaux (Beauvais, 1991). Both hydrodynamical and hypothetical biophysical processes control redox conditions which determine the trace element behaviour and their relation to lateritic minerals. Thus, this could explain that Ti, Zr and Nb are depleted in protopisolithic and vermiform ferricretes, while Ba, Ce and Co are correlated to Mn-oxyhydroxides. This geochemical association is common in lateritic soils (Taylor, 1968; Childs, 1975) evolving under limited geochemical conditions of Eh and pH (Parc et al., 1989; Braun et al., 1990). However, outside those conditions, Mn is depleted, and a correlation between Ba, Ce, Sr and La appears, reflecting unweathered relics of micas and feldspars.

Therefore, we are inclined to infer that the actual distribution of ferricrete in the Haut-Mbomou region is the result of a long time evolution of complex weathering and geomorphic processes driven by the downward reduction of the regolith along with climatic evolution from past-drier to actual-wetter conditions. In turn, that leads to the progressive disappearance of high plateau ferricretes, and hence, to the loss of parent rock signatures.

7. Conclusion

Our results indicate that the regional distribution of different ferricrete facies developed on tectonically stable cratons reflects the interplay between weathering and erosion processes of thick and old lateritic profiles rather than any variety of parent rocks. Petrological and geomorphological patterns of ferricrete facies as well as the behaviour of trace elements among the different minerals sustain this interpretation revealing that high plateau ferricretes could be the oldest, still preserving some geochemical signature of amphibole schists. If so, the hillslopes and low plateaux ferricrete facies might be younger, deriving from a long time evolution of the landscape under the effects of hydroclimatic and geomorphic changes, that tend to blur the parent rock inheritance. Although we do not deny the role of parent rock in the first stage of development of lateritic weathering profiles, we also believe that variations of climatic and geomorphic processes over several million years may influence both the regional distribution and petrological pattern of many old ferricretes widespread on ancient tropical shields.

Acknowledgements

This work was supported by the "Institut Français de Recherche Scientifique pour le Développement en Coopération" and the research program PIRAT (ORSTOM/INSU-

CNRS). We thank the "Centre de Géochimie de la Surface" at the University of Strasbourg (France) for mineralogical and geochemical analyses. The first author is indebted to the "Laboratoire de Pétrologie de la Surface" at the University of Poitiers for facilities in preparing a previous version of this paper. We also thank Vincent Eschenbrenner and Boris Volkoff for helpful critiques of a manuscript draft. Discussions with Dr. Yves Boulvert are appreciated. Dr. Kroonenberg and Dr. Franzmeier are also acknowledged for their useful critiques on the paper.

References

- Ambrosi, J.P. and Nahon, D., 1986. Petrological and geochemical differentiation of lateritic iron crust profiles. *Chem. Geol.*, 57: 371–393.
- Beauvais, A., 1991. Paléoclimats et dynamique d'un paysage cuirassé du Centrafrique. Morphologie, Pétrologie et Géochimie. Ph.D. Thesis, Univ. Poitiers. 317 pp. (microfilmed).
- Beauvais, A. and Colin, F., 1993. Formation and transformation processes of iron duricrust systems under tropical humid environment. *Chem. Geol.*, 106: 77–101.
- Beauvais, A. and Tardy, Y., 1993. Degradation and dismantling of iron crusts under climatic changes in Central Africa. *Chem. Geol.*, 107: 277–280.
- Boeglin, J.L. and Mazaltarim, D., 1989. Géochimie, degrés d'évolution et lithodépendance des cuirasses ferrugineuses de la région de Gaoua au Burkina-Faso. *Sci. Géol. Bull. Strasbourg*, 42: 27–44.
- Boski, T. and Herbosch, A., 1990. Trace elements and their relation to the mineral phases in the lateritic bauxites from southeast Guinea Bissau. *Chem. Geol.*, 82: 279–297.
- Boulvert, Y., 1976. Type de modelé cuirassé. Intérêt morphopédologique des "lakérés". Finesse, précision de la télédétection. Relations avec le tapis végétal (région de Dembia). *Rev. Photo Interprétation, Technip, Paris*. Vol. 4, pp. 18–29.
- Boulvert, Y., 1986. Carte phytogéographique de la République Centrafricaine à 1/1 000 000. ORSTOM, Paris, Notice Explicative No. 104. 132 pp.
- Boulvert, Y., 1996. Etude géomorphologique de la République centrafricaine. Carte à 1/1 000 000 en deux feuilles ouest et est. Thèse Univ., Dijon. Notice Explicative No. 110. ORSTOM, Paris, 259 pp.
- Braun, J.J., Pagel, M., Muller, J.P., Bilong, P., Michard, A. and Guillet, B., 1990. Cerium anomalies in lateritic profiles. *Geochim. Cosmochim. Acta*, 54: 781–795.
- Brimhall, G.H. and Dietrich, W.E., 1987. Consecutive mass balance relations between chemical composition, volume, density, porosity, and strain in metasomatic hydrochemical systems: results on weathering and pedogenesis. *Geochim. Cosmochim. Acta*, 51: 567–587.
- Butt, C.R.M., 1987. A basis for geochemical exploration models for tropical terrains. *Chem. Geol.*, 60: 5–16.
- Butt, C.R.M. and Zeegers, H., 1989. Classification of geochemical exploration models for tropically weathered terrains. *J. Geochem. Explor.*, 32: 65–74.
- Childs, C.W., 1975. Composition of iron–manganese concretions from New-Zealand soils. *Geoderma*, 13: 141–152.
- Colin, F. and Vieillard, P., 1991. Behaviour of gold in the lateritic environment: weathering and surface dispersion of residual gold particles, at Dondo Mobi, Gabon. *Appl. Geochem.*, 6: 279–290.
- Colin, F., Brimhall, G.H., Nahon, D., Lewis, C.J., Baronnet, A. and Danti, K., 1992. Equatorial rain forest lateritic mantles: a geomembrane filter. *Geology*, 20: 523–526.
- Davies, T.C. and Bloxham, T.W., 1979. Heavy metal distribution in laterites, southwest of regent, Freetown igneous complex, Sierra Leone. *Econ. Geol.*, 74(3): 638–644.
- Delvigne, J., 1965. Pédogenèse en zone tropicale. La formation des minéraux secondaires en milieu ferrallitique. *Mém. ORSTOM, Paris*, Vol. 13, 177 pp.
- Donkin, M.J. and Fey, M.V., 1991. Factor analysis of familiar properties of some Natal soils with potential for afforestation. *Geoderma*, 48(3/4): 297–304.
- Eschenbrenner, V., 1987. Les glébules des sols de Côte d'Ivoire. Thèse ès Sci., Univ. Bourgogne, Dijon, 496 pp. (unpublished).

- Franquin, P., Diziain, P., Cointepas, J.P. and Boulvert, Y., 1988. Agroclimatologie du Centrafrique. Coll. Init. Docum. Techniques, ORSTOM, Paris, Vol. 71, 522 pp.
- Freyssinet, P., 1990. Géochimie et minéralogie des latérites du sud-Mali. Evolution des paysages et prospection géochimique de l'or. Ph.D. Thesis, Univ. Strasbourg, Mém. B.R.G.M., Orléans, Vol. 203, 269 pp.
- Freyssinet, P., Lecomte, P. and Edimo, F., 1989. Dispersion of gold and base metals in the Mborguéné lateritic profile, East Cameroun. *J. Geochem. Explor.*, 31: 99–116.
- Kämpf, N. and Schwertmann, U., 1983. Goethite and hematite in climosequence in southern Brazil and their application in classification of kaolinitic soils. *Geoderma*, 29: 27–41.
- Lebart, L., Morineau, A. and Fénélon, J.P., 1979. Traitement des données statistiques. Dunod, Paris, 510 pp.
- Lecomte, P. and Colin, F., 1989. Gold dispersion in a tropical rainforest weathering profile at Dondo Mabi, Gabon. *J. Geochem. Explor.*, 34: 285–301.
- Leprun, J.C., 1979. Les cuirasses ferrugineuses des pays cristallins de l'Afrique occidentale sèche. Genèse. Transformation. Dégradation. Mém. Sci. Géol. Strasbourg, Vol. 58, 224 pp.
- Litaor, M.I., Dan, Y. and Koyumdjisky, H., 1989. Factor analysis of a lithosequence in the northeastern Samaria steppe (Israel). *Geoderma*, 44: 1–15.
- Matheis, G., 1981. Trace element patterns in lateritic soils applied to geochemical exploration. *J. Geochem. Explor.*, 15(1–3): 471–480.
- Matheis, G. and Pearson, M.J., 1982. Mineralogy and geochemical dispersion in lateritic soil profiles of northern Nigeria. *Chem. Geol.*, 35: 129–145.
- Mazaltarim, D., 1989. Géochimie des cuirasses ferrugineuses et bauxitiques de l'Afrique de l'Ouest et Centrale. Ph.D. Thesis, Univ. Strasbourg, 260 pp. (unpublished).
- Mestraud, J.P., 1982. Géologie et ressources minérales de la République Centrafricaine. Etat des connaissances fin 1963. Mém. B.R.G.M., Orléans, Vol. 60, 185 pp.
- Millot, G., 1970. Geology of Clays. Springer Verlag, Heidelberg, 429 pp.
- Mosser, C., 1980. Etude géochimique de quelques éléments traces dans les argiles des altérations et des sédiments. *Sci. Géol. Mém., Strasbourg*, Vol. 63, 229 pp.
- Nahon, D., 1976. Cuirasses ferrugineuses et encroûtements calcaires au Sénégal occidental et en Mauritanie. Systèmes évolutifs: géochimie, structures, relais et coexistence. *Sci. Géol. Mém. Strasbourg*, Vol. 44, 232 pp.
- Nahon, D., 1986. Evolution of iron crusts in tropical landscapes. In: S.M. Coleman and D.P. Dethier (Editors), Rates of Chemical Weathering of Rock and Minerals. Academic Press, pp. 169–191.
- Nahon, D.B., 1991. Introduction to the Petrology of Soils and Chemical Weathering. Wiley, New York, 313 pp.
- Nalovic, L., 1977. Recherches géochimiques sur les éléments de transition dans les sols. Etude expérimentale de l'influence des éléments traces sur le comportement du fer et l'évolution des composés ferriques au cours de la pédogenèse. *Trav. Doc. ORSTOM, Paris*, Vol. 66, 235 pp.
- Parc, S., Nahon, D., Tardy, Y. and Vieillard, P., 1989. Estimated solubility products and fields of stability for cryptomelane, nsutite, bimessite and lithiophorite based on natural lateritic weathering sequences. *Am. Mineral.*, 74: 466–475.
- Roquin, C., Dandjinou, T., Freyssinet, P. and Pion, J.C., 1989. The correlation between geochemical data and spot satellite imagery of lateritic terrain in Southern Mali. *J. Geochem. Explor.*, 32: 149–168.
- Roquin, C., Freyssinet, P., Zeegers, H. and Tardy, Y., 1990. Element distribution patterns in laterites of southern Mali: consequence for geochemical prospecting and mineral exploration. *Appl. Geochem.*, 5: 303–315.
- SAS (Statistical Analysis System), 1985. User's Guide: Statistics, Version 5. SAS Inst. Inc., Cary, NC, 956 pp.
- Schwertmann, U. and Taylor, R.M., 1977. Iron oxides. in: J.B. Dixon, S.B. Weed, J.A. Kittrick, M.H. Milford and J.L. White (Editors), Minerals in Soil Environments. Soil Science Society of America, Madison, WI, pp. 145–180.
- Tardy, Y., 1969. Géochimie des altérations. Etude des arènes et des eaux de quelques massifs cristallins d'Europe et d'Afrique. Mém. Serv. Carte Géol., Als. Lorr., Strasbourg, Vol. 31, 199 pp.
- Tardy, Y., 1993. Pérologie des Latérites et des Sols Tropicaux. Masson, Paris, 535 pp.
- Tardy, Y. and Nahon, D., 1985. Geochemistry of laterites, stability of Al-goethite, Al-hematite, and

- Fe³⁺-kaolinite in bauxites and ferricretes: an approach to the mechanism of concretion formation. *Am. J. Sci.*, 285: 865–903.
- Tardy, Y., Mazaltarim, D., Boeglin, J.L., Roquin, C., Pion, J.C., Paquet, H. and Millot, G., 1988a. Lithodépendance et homogénéisation de la composition minéralogique et chimique des cuirasses ferrugineuses latéritiques. *C.R. Acad. Sci. Paris Sér. II*, 307: 1765–1722.
- Tardy, Y., Melfi, A.J. and Valetton, I., 1988b. Climats et paleoclimats tropicaux périallantiques. Rôle des facteurs climatiques et thermodynamiques: température et activité de l'eau sur la répartition et la composition minéralogique des bauxites et des cuirasses ferrugineuses, au Brésil et en Afrique. *C.R. Acad. Sci. Paris Sér. II*, 306: 289–295.
- Tardy, Y., Kolbisek, B. and Paquet, H., 1991. Mineralogical composition and geographical distribution of African and Brazilian periatlantic laterites. The influence of continental drift and tropical paleoclimates during the past 150 million years and implications for India and Australia. *J. Afr. Earth Sci.*, 12(1/2): 283–295.
- Taylor, R.M., 1968. The association of Mn and Co in soils. Further observations. *J. Soil. Sci.*, 19: 77–80.
- Trescases, J.J., 1975. L'évolution géochimique supergène des roches ultrabasiqes en zone tropicale. Formation des gisements nickélicifères de Nouvelle-Calédonie. *Mém. ORSTOM, Paris*, Vol. 78, 259 pp.
- Zeegers, H. and Leprun, J.C., 1979. Evolution des concepts en altérogénie tropicale et conséquences potentielles pour la prospection géochimique en Afrique occidentale soudano-saharienne. *Bull. B.R.G.M. Orléans*, 2(2/3): 222–239.

Note to Contributors

A detailed Guide for Authors is available upon request. Please pay special attention to the following notes:

Language

Manuscripts should be written in English. Authors whose native language is not English are recommended to seek the advice of a colleague who has English as his mother-tongue before submitting their manuscript.

Authors in Japan please note: Upon request, Elsevier Science Japan will provide authors with a list of people who can check and improve the English of their paper (*before submission*). Please contact our Tokyo office: Elsevier Science Japan, 1-9-15 Higashi-Azabu, Minato-ku, Tokyo 106; Tel. +81 5 5561 5032; Fax +81 5 5561 5045.

Preparation of the text

(a) The manuscript should preferably be prepared on a word processor and printed with double spacing and wide margins and include an abstract of not more than 500 words. (b) Authors should use IUGS terminology. The use of S.I. units is also recommended. (c) The title page should include the name(s) of the author(s), their affiliations, fax and e-mail numbers. In case of more than one author, please indicate to whom the correspondence should be addressed.

Keywords

Except for the journals *Coastal Engineering* and *Hydrometallurgy*, authors should provide 4 to 6 keywords. These must be taken from the most recent American Geological Institute GeoRef Thesaurus and should be placed beneath the abstract. *Hydrometallurgy* authors will be provided with a list of keywords by the editor upon submission of manuscripts.

References

References in the text consist of the surname of the author(s), followed by the year of publication in parentheses. All references cited in the text should be given in the reference list and vice versa.

Tables

Tables should be compiled on separate sheets and should be numbered according to their sequence in the text. Tables can also be sent as glossy prints to avoid errors in typesetting.

Illustrations

(a) All illustrations should be numbered consecutively and referred to in the text. (b) Colour figures can be accepted providing the reproduction costs are met by the author. Please consult the publisher for further information.

Page proofs

One set of page proofs will be sent to the corresponding author, to be checked for typesetting/editing. The author is not expected to make changes or corrections that constitute departures from the article in its accepted form. Proofs should be returned within 3 days.

Reprints

Fifty reprints of each article are supplied free of charge. Additional reprints can be ordered on a reprint order form which will be sent to the corresponding author upon receipt of the accepted article by the publisher.

Submission of manuscripts

Three copies should be submitted to: Editorial Office Geoderma, P.O. Box 1930, 1000 BX Amsterdam, The Netherlands. Illustrations: Please note that upon submission of a manuscript THREE SETS of all photographic material printed SHARPLY on GLOSSY PAPER or as HIGH-DEFINITION LASER PRINTS must be provided to enable meaningful review. Photocopies and other low-quality prints will not be accepted for review. The indication of a fax and e-mail number on submission of the manuscript could assist in speeding communications. The fax number for the Amsterdam office is +31-20-4852696. Submission of an article is understood to imply that the article is original and unpublished and is not being considered for publication elsewhere. Authors are requested to submit, with their manuscripts, the names and addresses of four potential referees.

Submission of electronic text

Authors are requested to submit the final text on a 3.5" or 5.25" diskette. It is essential that the name and version of the word processing program, the type of computer on which the text was prepared, and the format of the text files are clearly indicated. Authors are requested to ensure that the contents of the diskette correspond exactly to the contents of the hard copy manuscript. If available, electronic files of the figures should also be included on a separate floppy disk.

Copyright © 1996 Elsevier Science B.V. All rights reserved.

0016-7061/96/\$15.00

This journal and the individual contributions contained in it are protected by the copyright of Elsevier Science B.V., and the following terms and conditions apply to their use:

Photocopying – Single photocopies of single articles may be made for personal use as allowed by national copyright laws. Permission of the Publisher and payment of a fee is required for all other photocopying, including multiple or systematic copying, copying for advertising or promotional purposes, resale, and all forms of document delivery. Special rates are available for educational institutions that wish to make photocopies for non-profit educational classroom use.

In the USA, users may clear permissions and make payment through the Copyright Clearance Center Inc., 222 Rosewood Drive, Danvers, MA 01923, USA. In the UK, users may clear permissions and make payment through the Copyright Licensing Agency Rapid Clearance Service (CLARCS), 90 Tottenham Court Road, London W1P 0LP, UK. In other countries where a local copyright clearance centre exists, please contact it for information on required permissions and payments.

Derivative works – Subscribers may reproduce tables of contents or prepare lists of articles including abstracts for internal circulation within their institutions. Permission of the Publisher is required for resale or distribution outside the institution. Permission of the Publisher is required for all other derivative works, including compilations and translations.

Electronic storage – Permission of the Publisher is required to store electronically any material contained in this journal, including any article or part of an article. Contact the Publisher at the address indicated.

Except as outlined above, no part of this publication may be reproduced, stored in a retrieval system or transmitted in any form or by any means, electronic, mechanical, photocopying, recording or otherwise, without prior written permission of the Publisher.

Notice – No responsibility is assumed by the Publisher for any injury and/or damage to persons or property as a matter of products liability, negligence or otherwise, or from any use or operation of any methods, products, instructions or ideas contained in the material herein.

Although all advertising material is expected to conform to ethical (medical) standards, inclusion in this publication does not constitute a guarantee or endorsement of the quality or value of such product or of the claims made of it by its manufacturer.

© The paper used in this publication meets the requirements of ANSI/NISO Z39.48-1992. (Permanence of Paper).

PRINTED IN THE NETHERLANDS

Volcanic Ash Soils

Genesis, Properties and Utilization

by S. Shoji, M. Nanzyo and R.A. Dahlgren

Developments in Soil Science Volume 21

Volcanic eruptions are generally viewed as agents of destruction, yet they provide the parent materials from which some of the most productive soils in the world are formed. The high productivity results from a combination of unique physical, chemical and mineralogical properties. The importance and uniqueness of volcanic ash soils are exemplified by the recent establishment of the Andisol soil order in Soil Taxonomy. This book provides the first comprehensive synthesis of all aspects of volcanic ash soils in a single volume. It contains in-depth coverage of important topics including terminology, morphology, genesis, classification, mineralogy, chemistry, physical properties, productivity and utilization. A wealth of data (37 tables, 81 figures, and Appendix) mainly from the Tohoku University Andisol Data

Base is used to illustrate major concepts. Twelve color plates provide a valuable visual-aid and complement the text description of the world-wide distribution for volcanic ash soils. This volume will serve as a valuable reference for soil scientists, plant scientists, ecologists and geochemists interested in biogeochemical processes occurring in soils derived from volcanic ejecta.

Short Contents:

1. Terminology, Concepts and Geographic Distribution of Volcanic Ash Soils.
2. Morphology of Volcanic Ash Soils.
3. Genesis of Volcanic Ash Soils.
4. Classification of Volcanic Ash Soils.



ELSEVIER
SCIENCE B.V.

5. Mineralogical Characteristics of Volcanic Ash Soils.
6. Chemical Characteristics of Volcanic Ash Soils.
7. Physical Characteristics of Volcanic Ash Soils.
8. Productivity and Utilization of Volcanic Ash Soils. Appendices. References Index. Subject Index.

1993 312 pages
Dfl. 290.00
(US \$ 165.75)
ISBN 0-444-89799-2

Elsevier Science B.V.
P.O. Box 1930
1000 BX Amsterdam
The Netherlands

P.O. Box 945
Madison Square Station
New York
NY 10160-0757

The Dutch Guilder (Dfl.) prices quoted apply worldwide. US \$ prices quoted may be subject to exchange rate fluctuations. Customers in the European Community should add the appropriate VAT rate applicable in their country to the price.